Thin Films from Atomic Layer Deposition for Membranes, Metamaterials, and Micromachines

CNF Project Number: 900-00

Principal Investigators: Paul McEuen[1], Itai Cohen[1]

Users: Kyle Dorsey[2], Tanner Pearson[2], Edward Esposito[1], Baris Bircan[2], Helen Xu[3]

Affiliations: 1. Laboratory of Atomic and Solid State Physics, 2. School of Applied and Engineering Physics, 3. Sibley School of Mechanical and Aerospace Engineering; Cornell University, Ithaca, NY

Primary Source of Research Funding: AFOSR MURI Grant FA2386-13-1-4118, NSF Grant DMR-1435829, (NSF) Major Research Instrumentation Award DMR-1429155 Kavli Institute at Cornell for Nanoscale Science CCMR Shared Facilities through the NSF MRSEC program (DMR-1719875)

Contact: plm23@cornell.edu, itai.cohen@cornell.edu, kjd96@cornell.edu, tgp34@cornell.edu, epe3@cornell.edu, bb625@cornell.edu, yx85@cornell.edu

Primary CNF Tools Used: Oxford FlexAL ALD, Arradiance ALD, Autostep AS200 i-line stepper, CVC e-beam evaporators, Oxford 81/82 etchers, PT770 and PT740 etchers, Anatech Asher, Zeiss SEMs, Veeco atomic force microscope, Tencor P7 profilometer, Filmetrics UV, Woollam ellipsometer, DISCO dicing saw, Heidelberg DWL2000

Abstract:

Ultra-thin films of inorganic materials are well-suited for fabrication of micron-scale actuators because they can sustain small radii of curvature, have large force outputs, are compatible with semiconductor processing, and are chemically robust. We leverage atomic layer deposition (ALD) on sacrificial substrates to produce micron-scale free-standing mechanical devices with sub-5 nm film thicknesses. We fabricate cantilever springs from ALD films and characterize the material's bending stiffness and elastic properties. We find values for the bending stiffness that are consistent with expectations from elasticity theory. The mechanical properties of ALD are further modified by lithographic patterning of the ALD. Lattices imposed into the film decrease its effective Young's modulus. We integrate these results and device concepts to produce magnetically actuated three-dimensional devices with applications in micromachinery. Our results establish thin ALD films as a scalable basis for micron-scale actuators and robotics.

Summary of Research:

Self-folding is a strategy for producing both static and dynamic three-dimensional devices from two-dimensional sheets at all size scales [1,2]. This conceptual framework is particularly well suited to the fabrication of micron-scale machinery because the dominant mode of manufacturing microscopic features is two-dimensional lithography. Folding therefore enables production of three dimensional parts by lithography. Furthermore, process integration with electronics fabrication is retained in this approach.

The relevant energy scale for design of micro-actuators is the actuator's bending stiffness. Micro-actuators that produce large deflections for small energy inputs must be made out of a material with low bending stiffness. Our approach is to scale hard materials to atomic-scale thicknesses [3-5]. In this work, we demonstrate that sub-10 nm thin films produced by atomic layer deposition (ALD) can serve as the backbone of small machinery.

We fabricate mechanical devices using ALD on films of aluminum, as is described in Figure 1. The aluminum serves as a sacrificial layer that can be undercut during wet-etching in dilute developer solution to release completed devices from the fabrication substrate. We manipulate devices in aqueous environments with surfactants to avoid stiction between the films and the substrate.

We use optical forces supplied by an infrared laser to actuate cantilever beams fabricated from 5 nm thick films of SiO_2 (Figure 2a). Although these forces are very weak, they can produce large deflections in the beam because of the low spring constants achievable. A force-distance curve from a representative device (Figure 2b) shows reversible elastic behavior with a spring constant on the order of 10^{-8} N/m, over nine orders of magnitude lower than typical AFM cantilevers.

The tailorable elastic response of springs fabricated from thin ALD films inspires design of stretchable metamaterials composed of panels and hinges. Figure 3a shows a sheet with a triangular lattice patterned with metallic panels. The cut pattern is shown in the inset.

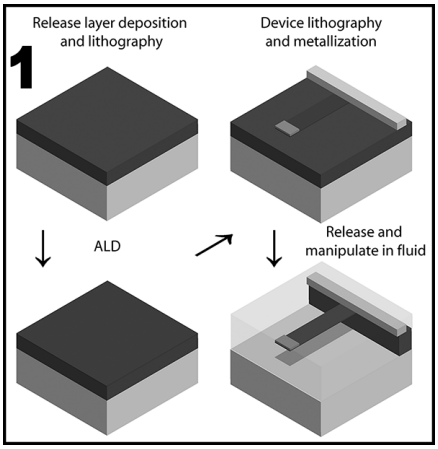

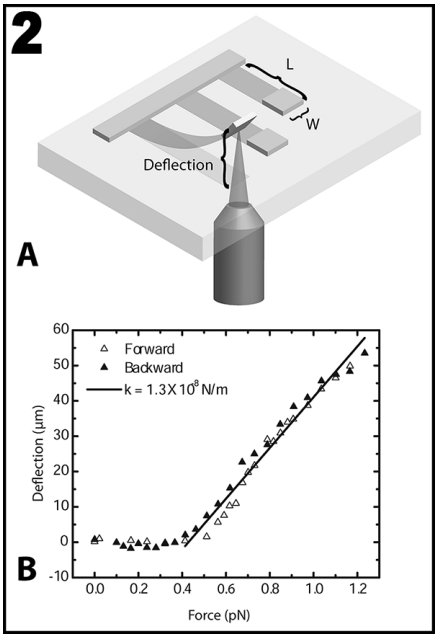

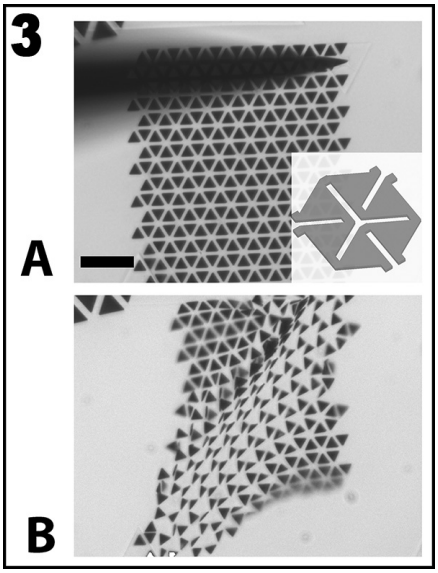

Figure 1, top: *Fabrication of free-standing films from atomic layer deposition.* ***Figure 2, middle:*** *Mechanical characterization of 5 nm thick films of SiO_2.* ***Figure 3, bottom:*** *Stretchable meta-materials fabricated from SiO_2 hinges (scale bar 30 μm).*

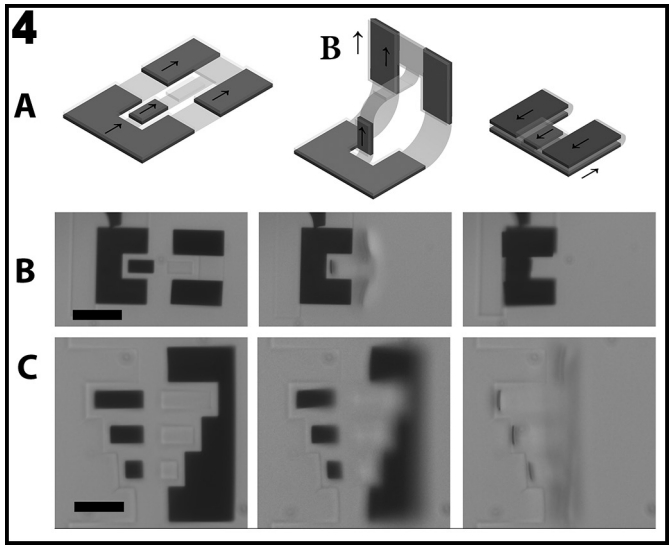

Figure 4: 3D magnetically actuated pop-up structures (scale 10μm).

Upon application of strain with a micromanipulator, the sheet can be stretched in both directions to ~ 100% beyond its original length without failure (Figure 3b).

We further manipulate these devices by patterning thin cobalt films to act as magnetic handles. A device concept is illustrated in Figure 4a. Application of external fields allow rotation of free hinges as shown in Figure 4a. Further rotation of the external field can close a latch structure formed with a second magnet. This concept is realized in Figure 4b, which shows a three-dimensional "pop-up" structure being rotated from the fabrication substrate into its 3D target geometry. It is then closed and remains shut. This simple design paradigm can be extended to more complicated 3D structures such as the micron-scale staircase shown in Figure 4c. We envision the materials and design concepts described herein to be used as the building blocks of more sophisticated 3D machinery at the micron scale.

References:

[1] Leong, Timothy G., Aasiyeh M. Zarafshar, and David H. Gracias. "Three-Dimensional Fabrication at Small Size Scales." Small 6, no. 7 (April 9, 2010): 792-806.

[2] Miskin, Marc Z., Kyle J. Dorsey, Baris Bircan, Yimo Han, David A. Muller, Paul L. McEuen, and Itai Cohen. "Graphene-Based Bimorphs for Micron-Sized, Autonomous Origami Machines." Proceedings of the National Academy of Sciences, January 1, 2018, 201712889.

[3] Davami, Keivan, Lin Zhao, Eric Lu, John Cortes, Chen Lin, Drew E. Lilley, Prashant K. Purohit, and Igor Bargatin. "Ultralight Shape-Recovering Plate Mechanical Metamaterials." Nature Communications 6 (December 3, 2015): 10019.

[4] Eigenfeld, Nathan T., Jason M. Gray, Joseph J. Brown, George D. Skidmore, Steven M. George, and Victor M. Bright. "Ultra-Thin 3D Nano-Devices from Atomic Layer Deposition on Polyimide." Advanced Materials 26, no. 23 (June 1, 2014): 3962-67.

[5] Wang, Luda, Jonathan J. Travis, Andrew S. Cavanagh, Xinghui Liu, Steven P. Koenig, Pinshane Y. Huang, Steven M. George, and J. Scott Bunch. "Ultrathin Oxide Films by Atomic Layer Deposition on Graphene." Nano Letters 12, no. 7 (July 11, 2012): 3706-10.

Graphene-Based Bimorphs for Micron-Sized Autonomous Machines

CNF Project Number: 900-00

Principal Investigators: Paul McEuen[a,b], Itai Cohen[a,b]

Users: Marc Miskin[a,b], Baris Bircan[c], Kyle Dorsey[c], Edward Esposito[a], Alejandro Cortese[c], Michael Reynolds[c]

Affiliations: a) Laboratory of Atomic and Solid State Physics, Cornell University, b) Kavli Institute at Cornell, c) Department of Applied and Engineering Physics, Department of Physics, Cornell University

Primary Sources of Research Funding: This work was supported by Cornell Center for Materials Research Grant DMR-1719875, National Science Foundation (NSF) Major Research Instrumentation Award DMR-1429155, NSF Grant DMR.1435829, Air Force Office of Scientific Research (AFSOR) multidisciplinary research program of the university research initiative Grant FA2386-13-1-4118, and the Kavli Institute at Cornell for Nanoscale Science

Contact: plm23@cornell.edu, ic64@cornell.edu, mm2325@cornell.edu

Primary CNF Tools Used: Oxford Flex ALD, Arradiance ALD, Oxford Cobra ICP etcher

Abstract:

We are developing origami into a tool for fabricating autonomous, cell-sized machines. In our approach, devices can interact with their environment, be manufactured en masse, and carry the full power of modern information technology. Our approach starts with origami in the extreme limit of folding 2D atomic membranes. We make actuators that bend to micron radii of curvature out of atomically thin materials, like graphene. By patterning rigid panels on top of these actuators, we can localize bending to produce folds, and scale down existing origami patterns to produce a wide range of machines. These machines change shape in fractions of a second in response to environmental changes, and perform useful functions on time and length scales comparable to microscale biological organisms. Beyond simple stimuli, we are currently developing voltage responsive actuators that can be powered by on-board photovoltaics. These new electronic actuation technologies are currently being combined with silicon-based electronics to create a powerful platform for robotics at the cellular scale.

Summary of Research:

Our group is shrinking down origami-robotics to become the fundamental platform for nanorobotics by folding atom's thick paper. In origami robotics, actuators, patterned on a sheet, are used to fold complex, reconfigurable 3D structures. This platform is prime for miniaturization because fabrication can be done in plane with tools like photolithography, designs are scale invariant, and flat panels linked by the folds provide a natural place to integrate electronics.

The most basic challenge to miniaturizing origami robots is in actuator design. A single actuator must be capable of bending to micron radii of curvature, produce force outputs large enough to lift embedded electronics, and maintain electrical conductivity across folds while bending. Through research conducted at the CNF, we have shown how actuation technologies based on atomic membranes, like graphene, can achieve these key functional requirements.

First, atomic origami devices can bend to micron radii of curvature using strains that are 100x smaller than the fracture strain for inorganic hard materials, thus maintaining electrical functionality across the actuator. Second, the devices are extremely stiff, capable of lifting the weight equivalent of a 500 nm thick silicon chip, enabling embedded electronics. Third, they can be fabricated and deployed en masse: 10 million devices fit on a 4-inch silicon wafer. Finally, devices can change shape from flat to folded in fractions of a second. Overall, the size, speed, stiffness and strength of these new actuators offer a new perspective on what is possible with nanoscale mechanical technology.

As our first prototypes, we designed and built actuators out of graphene and nanometer thick layers of glass.

These glass layers were deposited at CNF using the Oxford Flex atomic layer deposition tool. By patterning

2-μm-thick rigid panels on top of bimorphs, we were able to localize bending to the unpatterned regions to produce folds. Although only nanometers thick, the graphene glass bimorphs were able to lift these panels, the weight equivalent of a 500-nm-thick silicon chip. Using panels and bimorphs, we showed how to scale down existing origami patterns to produce a wide range of machines. We demonstrated that these machines were capable of changing shape in fractions of a second when crossing a tunable pH threshold.

Combined, the work developed a platform for building machines that sense their environments, respond, and perform useful functions on time and length scales comparable with microscale biological organisms.

Currently we are taking key steps in moving towards true robotic systems at the cellular scale by integrating nanoscale origami actuators with electronics. We are now capable of designing and building high efficiency actuators for self-folding machines that are powered by voltage. This advance relies on new metal atomic layer deposition capabilities through the CNF's Arradiance atomic layer deposition tool. These devices can be powered and controlled using standard CMOS electronic components like photovoltaics and transistors. As a first step, we are building basic prototypes that use on-board photovoltaics to power origami actuators. The resulting device can then change shape from flat to folded when external power is supplied through light fields. By combining this actuation technology with origami motifs, we are working to create a walking, autonomous robot no bigger than a few red blood cells in size.

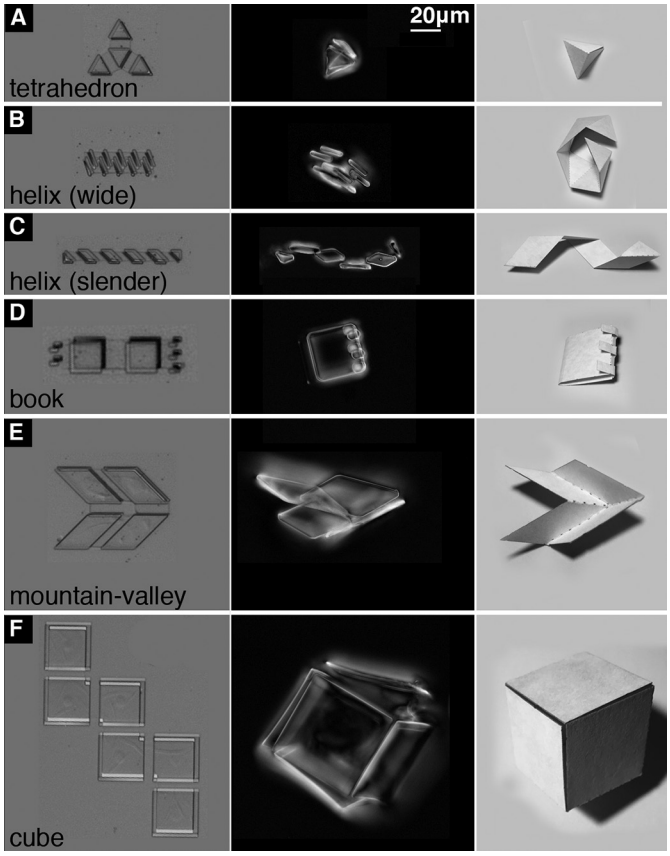

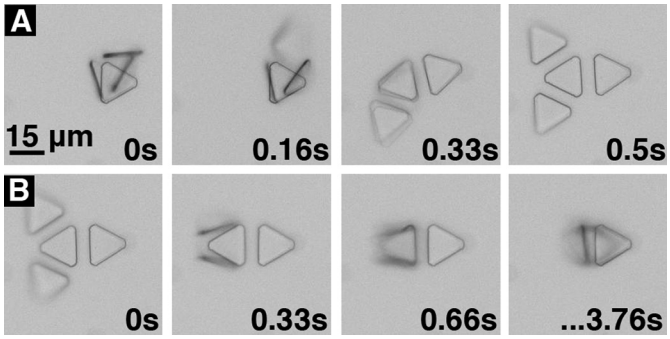

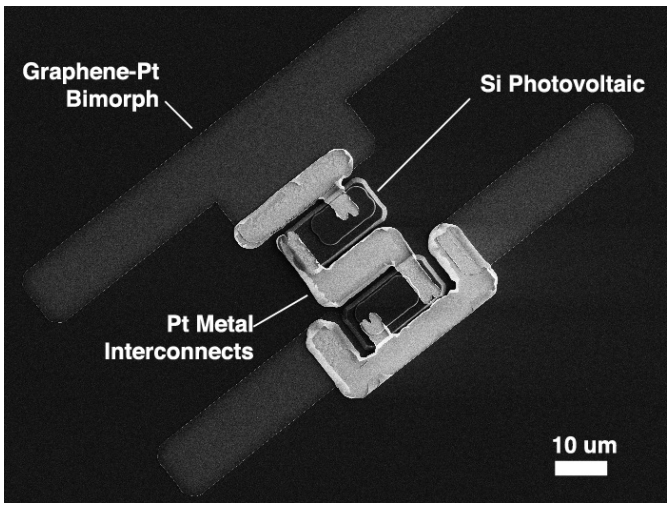

References:

[1] Miskin, et al., Graphene-based bimorphs for micron-sized, autonomous origami machines, PNAS, 2018.

Figure 1, top right: *Graphene origami can be used to fabricate numerous 3D structures at the micrometer scale. Shown here are tetrahedron (A), helices of controllable pitch (B and C), high-angle folds and clasps (D), basic origami motifs with bidirectional folding (E), and boxes (F). In Left, we show the device flattened and still attached to the release layer during fabrication. After the release layer is etched, the bimorphs self-assemble to their targeted 3D geometries (Center).* ***Figure 2, middle right:*** *Graphene origami devices are capable of rapid actuation due to the extreme slenderness of the working materials. Here a graphene origami tetrahedron changes shape from flat to folded and back in response to variations in local electrolyte content. The folding processes is fast, taking place in less than second.* ***Figure 3, bottom right:*** *A first prototype integrating a silicon based photovoltaic with atomic origami actuators. These origami actuators are capable of transforming from flat to folded by applying a voltage of only a few hundred millivolts and nanowatts of power. The photovoltaics supply rough 3x more voltage than is needed and roughly three orders of magnitude more power. The resulting machine will be capable of walking to explore its environment, fully untethered, using the actuators for locomotion and the photovoltaics for power.*

NEMS Electrostatic Switch for Near Zero Power RF Wakeup

CNF Project Number: 1262-04

Principal Investigator: Amit Lal

User: Alexander Ruyack

Affiliation: Electrical and Computer Engineering, Cornell University

Primary Sources of Research Funding: Defense Advanced Research Projects Agency (DARPA) project; Near Zero Power RF and Sensor Operations (N-ZERO)

Contact: amit.lal@cornell.edu, arr68@cornell.edu

Primary CNF Tools Used: ASML 300C DUV stepper, Heidelberg DWL2000, Gamma automatic coat-develop tool, Zeiss Ultra SEM, Zeiss Supra SEM, Oxford 81, 82, and 100 etchers, AJA ion mill, Hamatech hot piranha, Primaxx vapor HF etcher, Plasma-Therm deep Si etcher, Uniaxis 770 deep Si etcher, DISCO dicing saw, wire bonder, Aura 100, Zygo

Abstract:

A near zero-power laterally actuated nanoelectromechanical systems (NEMS) electrostatic radio frequency (RF) switch with multi-gate DC tunable threshold is presented as a portion of an overall wireless sensor node with less than 10 nW power consumption. Previously these switches were demonstrated as means of signal detection from a suite of zero power sensors. Various design updates and fabrication improvements have since been implemented to reach the desired -100 dBm RF sensitivity. The addition of folded trusses, compliant contacts and selections in contact material allow the device to be operated at resonance and reduce bending and variation, improving performance and reducing failure rate. Furthermore, processing with the Plasma-Therm Versaline deep reactive ion etch (DRIE) tool has resulted in 300 nm features within 5% of the drawn dimensions in CAD.

Introduction:

Sensor node reliability is limited by the longevity of the energy sources used to power them [1]. In order to maximize the sensor node operation time, power consumption by all components must be minimized. The power consumed by the sensors of the sensor node is especially critical because the sensors must operate all the time to generate a wakeup trigger for the digital and communication components. Previously, we demonstrated MEMS inertial, magnetic and acoustic sensors made of piezoelectric materials, which promise sensing without any power consumption [2]. These sensors, in conjunction with NEMS switches [3] showed successful classification of a portable electrical generator in different operation modes (on, off, eco) [4]. However, since these sensor nodes are wireless, detection of an RF wake-up signal is equally important and there must be an asleep-yet-aware detection method for RF signals. For this, we used the NEMS switch again with a reworked design and fabrication process in order to achieve the desired -100 dBm sensitivity.

Summary of Research:

A single photomask process is used to fabricate the NEMS switches on a silicon-on-insulator (SOI) substrate. Previously, alumina was used as a hard mask for a reactive ion etch (RIE) with subsequent alumina etch, metal deposition for conductivity, and release with wet hydrofluoric acid (HF) via critical point drying or vapor HF. This process resulted in over etched features, significant scalloping and large out of plane bending of released devices. By moving to a photoresist (PR)-only process with the Plasma-Therm VersaLine DRIE tool, the over-etching was minimized, scalloping reduced to < 20 nm, and out of plane bending minimized. Furthermore, additional design modifications were made to help push the sensitivity of the switch to -100 dBm. Folded springs and trusses help reduce bending and a compliant contact helps reduce contact lifetime and resistance. Additionally, smaller gaps were achievable with the new process, increasing the electrostatic force and helping sensitivity. Figure 1 shows a top down micrograph of a finished, unreleased device.

Figure 2 is a micrograph showing a 350 nm contact gap measurement. DRIE scallops can be seen on the left side of the image within the two release holes. The Figure 2 inset shows a Zygo white light interferometry image showing the out of plane bending of a released device. At the contact, there is a 30 nm out of plane displacement,

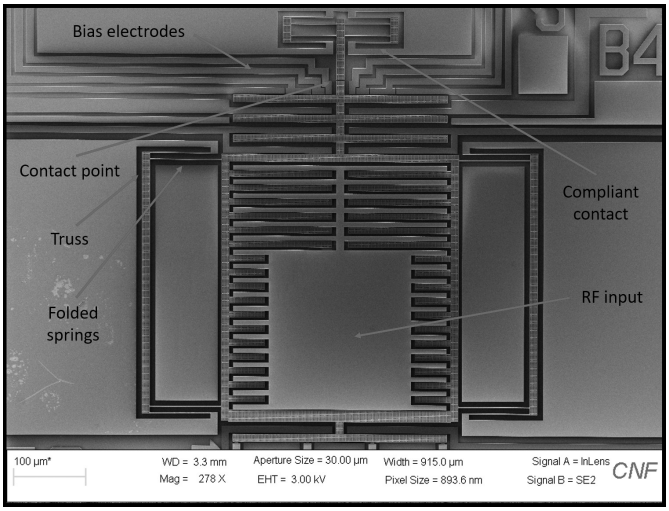

Figure 1: SEM micrograph of NEMS switch from above showing important electrical contacts and features.

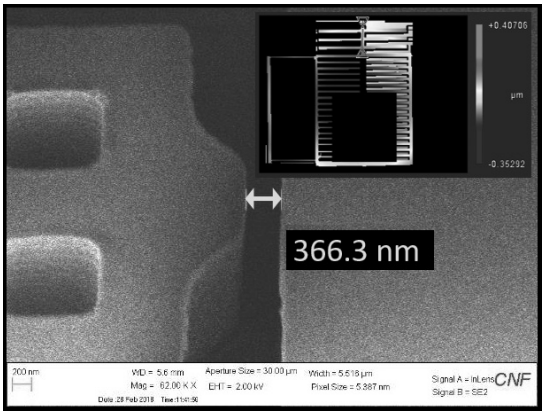

Figure 2: SEM micrograph with contact gap measurement. (Inset) Zygo optical profilometry measurement of out-of-plane bending of released device.

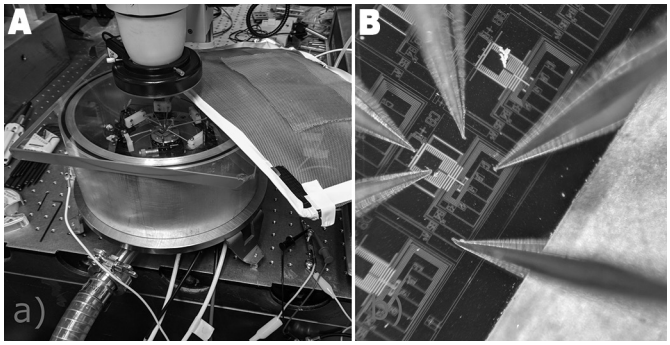

Figure 3: (a) Custom vacuum probe station. (b) Example image of device under test in probe station.

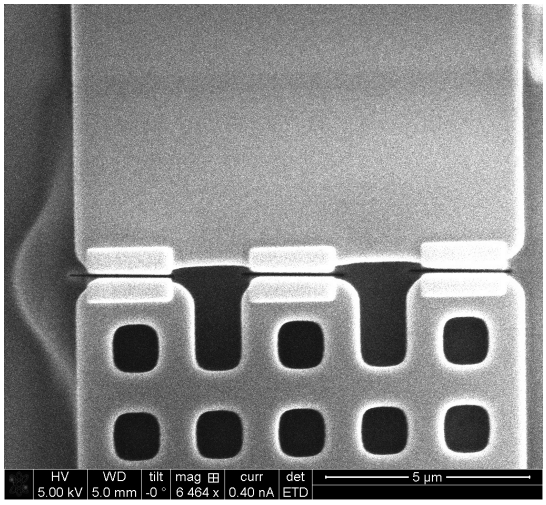

Figure 4: SEM micrograph after FIB Pt deposition and subsequent cutting with ion beam, resulting in near 100 nm gap.

which is small compared to the 2 μm device layer and 1 μm oxide layer.

Testing was done in a custom-built vacuum probe station (Figure 3a). An example image of a device under test can be seen in Figure 3b. Testing is currently underway for probability of detection (POF) and false alarm rate (FAR) using a high gain low noise Stanford Research Systems 570 TIA for detection, Keithley 2400s for biasing and a Rhode and Schwarz SMC100A RF signal generator.

Additional work still needs to be done to ensure reliable and repeatable contacting of the device. Efforts are underway to coat the contact interfaces with platinum (Pt) using a focused ion beam (FIB). Figure 4 shows an example device contact area (with three contact points) that has been completely covered with Pt and then re-cut with the ion beam to form approximately 100 nm contact gaps. There is also additional work being done to translate these devices to an out-of-plane design instead of in-plane. These devices are made via a flip-chip bonding process between a similar SOI chip and patterned lithium niobate ($LiNbO_3$ or LN) chip with graphene. These devices have the advantage of much larger electrostatic area (for better sensitivity) and RF filtering capabilities on the LN.

References:

[1] J. Yick, B. Mukherjee, and D. Ghosal. "Wireless sensor network survey," Computer networks 52, no. 12 (2008): pp 2292-2330.

[2] S. K. Gupta, V. Pinrod, S. Nadig, B. Davaji and A. Lal. "Vibration Powered RF-Transponder for Sensing Low Frequency Motion Events," PowerMEMS 2016.

[3] K. Amponsah, N. Yoshimizu, S. Ardanuc, and A. Lal, "Near-kT switching-energy lateral NEMS switch," IEEE NEMS 2010, pp. 985-988.

[4] V. Pinrod, A. Ruyack, R. Ying, B. Davaji, A. Molnar, A. Lal, "PZT Lateral Bimorph Based Sensor Cuboid for Near Zero Power Sensor Nodes," IEEE Sensors 2017.

Origin of Microlayer in Pool Boiling

CNF Project Number: 2123-12

Principal Investigator: Shalabh C. Maroo

Users: An Zou, Manish Gupta

Affiliation: Department of Mechanical and Aerospace Engineering, Syracuse University, Syracuse, NY 13244

Primary Sources of Research Funding: Startup funds from Department of Mechanical and Aerospace Engineering at Syracuse University; National Science Foundation Career Award NO. 1454450

Contact: scmaroo@syr.edu, azou@syr.edu and magupta@syr.edu

Website: http://maroo.syr.edu

Primary CNF Tools Used: CHA thermal evaporator, E-beam evaporator, CVC sputter, Oxford PECVD, GSI PECVD, Glen 1000 Plasma, Oxford 81/82 etcher

Abstract:

Microlayer evaporation is one of the major heat transfer mechanisms of boiling. In our work, the microlayer thin film is visualized *in situ* in a vapor bubble during pool boiling. Contrary to current understanding, bubbles originate on hydrophilic and silane-coated hydrophobic surfaces without a three-phase contact line, i.e. the microlayer completely covers the bubble base. The occurrence of such a wetted bubble base is found to be dependent on the liquid-solid interaction, which is validated by molecular dynamics simulations of nucleation of liquid argon on hydrophilic and/or single-layer hydrophobic atoms on hydrophilic surfaces. The work reported here is part of a journal article which is currently under review.

Summary of Research:

Microlayer is a thin liquid film trapped underneath a vapor bubble next to three-phase contact line. The base of the bubble can be divided into three regions: nanoscale non-evaporating film region, microscale evaporating film region, and millimeter scale bulk meniscus (Figure 1). Extremely high heat flux occurs in the microlayer region due to its low thermal resistance, which is proportional to liquid layer thickness. Microlayer evaporation serves as one of the major heat transfer mechanism. Better understanding of the microlayer has led to novel approaches for boiling heat transfer enhancement: microstructures fabricated on pool boiling surface causes early evaporation of microlayer, resulting in ~ 120% enhancement in the critical heat flux [1]. In our work, we studied origin of microlayer by *in situ* visualizing the microlayer in a vapor bubble in pool boiling, and performing molecular dynamics simulations of bubble nucleation.

We used laser heating to create a vapor bubble on a surface submerged in a pool of deionized (DI) water at room temperature. The surface consists of several metal layers for laser heating technology (Figure 2):a 40 nm thick tungsten was deposited on a glass substrate to absorb the laser and heat the surface; a 1 μm thick PECVD SiO_2 was deposited to serve as hydrophilic surface (contact angle: 33.4 ± 2.7°); two 10 nm thick Ti layers were deposited acting as adhesion layer. To form the vapor bubble, a blue CW laser beam (wavelength of 447 ± 5 nm) was introduced into an inverted microscope, passed through a 50× objective, and focused on the sample to generate a highly localized heating area corresponding to an equivalent beam diameter of ~ 15 μm. The same objective was used to image the bubble which was illuminated from above with a 632 nm HeNe laser. This configuration creates a bubble image with a dark annulus ring as light has to refract across multiple interfaces in that region. A high-speed camera was used to record the bubble formation process.

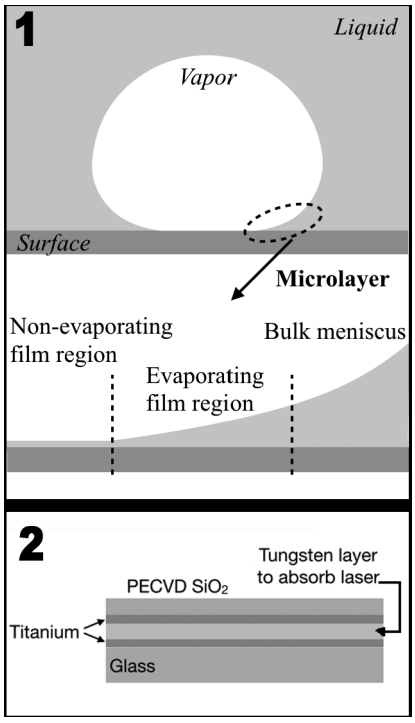

Figure 1, top: Microlayer underneath a vapor bubble in pool boiling. Figure 2, bottom: Sample surface with metal layers to absorb laser.

The microlayer is *in situ* visualized using this setup because fringes would be observed in microlayer region. These fringes were observed due to thin film interference of monochromatic incident light with partially reflected light within the thin liquid microlayer. As the generated dark and bright fringes correspond to constructive and destructive interference respectively, these fringes are separated by an optical path difference which is half wavelength, and the position of the fringes can be used to build microlayer profile.

In our experiments, the fringes are surprisingly seen throughout the bubble base on the surface, indicating that the microlayer liquid film covers entire bubble base and no three-phase contact line forms (Figure 3). In order to understand the physics behind the completely wetted bubble base, molecular dynamics simulations were performed in LAMMPS [2] software with liquid argon present between two walls. The upper wall was moved outward at a certain speed to decrease the pressure in the liquid and initiate nucleation. The lower wall was modeled as the hydrophilic surface by using a 12-2 Lennard Jones potential between the wall and argon atoms. Similar to the experiments, a liquid film is present between the bubble and the surface (Figure 4). Statistical analysis from molecular dynamics simulation shows that due to the strong interaction between the hydrophilic wall and argon atoms, high density liquid layers form near the wall, leading to significantly high pressure in that region. Thus, a bubble forms above these liquid layers as it is thermodynamically favorable to achieve lower pressures required for nucleation, resulting in a liquid film being present underneath the bubble. This mechanism can be amplified/weakened with different wall-liquid combinations, for e.g., interaction between SiO_2 and water were much stronger as polar atoms are involved, leading to thicker high-density liquid water film that is measurable in experiments. However, the completely wetted bubble base will not likely be observed on weak interacted wall-liquid combinations (if either is non-polar).

In summary, we observed that the bubble, at its early growth stage, had a bubble base that is completely covered by the microlayer; similar observation was found in molecular dynamics simulations. This entirely wetted bubble base is due to the strong wall-liquid interactions, the thickness of microlayer is determined by the wall-liquid interactions.

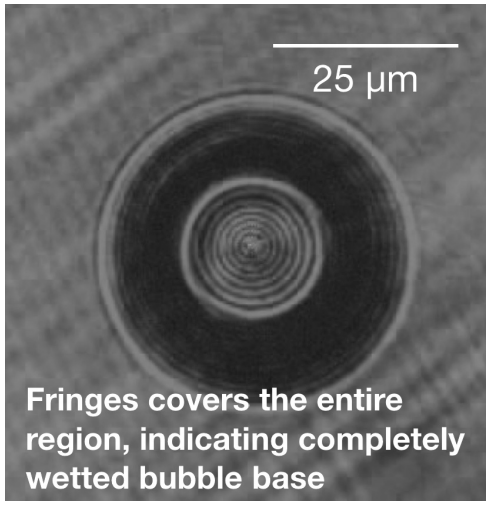

Figure 3: Image of a vapor bubble with completely wetted bubble base.

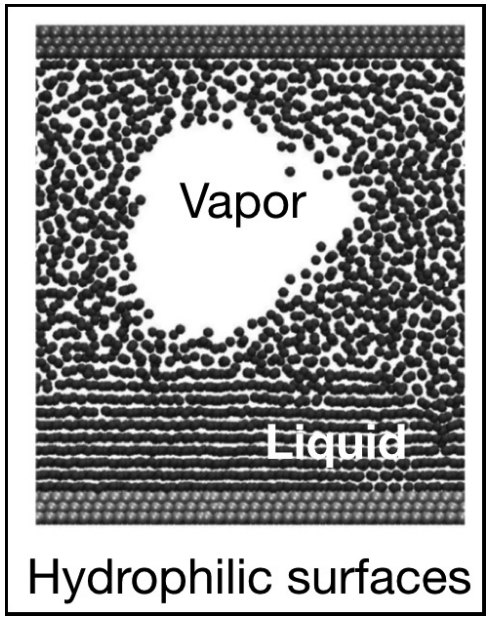

Figure 4: Bubble with completely wetted base in molecular dynamics simulation.

References:

[1] A. Zou, D. P. Singh, and S. C. Maroo, Langmuir 32, 10808-10814 (2016).

[2] S. Plimpton, J. Comput. Phys. 117, 1-19 (1995).

Making a Microfluidic Device to Mimic Flow Through Porous Medium

CNF Project Number: 2385-15

Principal Investigator: Brian Kirby

User: Katherine Polhemus

Affiliation: Sibley School of Mechanical and Aerospace Engineering, Cornell University

Primary Source of Research Funding: IGERT Program for Earth Energy

Contact: kirby@cornell.edu, kcp44@cornell.edu

Primary CNF Tools Used: CAD software L-Edit, photolithography tool set, ABM contact aligner, hot press, CorSolutions microfluidic probe station

Abstract:

With the rapid depletion of known oil reserves, detecting properties of the oil reservoirs and optimizing oil extraction is critical. By measuring the aqueous properties of the reservoirs, decisions can be made on which reservoirs to drill and the available quantity of oil to extract, with minimal environmental impact. Utilizing hairy nanoparticles in testing can provide a variety of information about the reservoir. The objective of the proposed work is to characterize the behavior of hairy nanoparticles at the oil-water interface in order to optimize their use as subsurface sensors. In order to complete the optimization, a microfluidic model for the environment needs to be developed. This past year's work involves making microfluidic devices to mimic water flowing through the subsurface and oil trapped in pores. The design and mold to make the mold was developed in the CNF first using photolithography to create a mold with negative photoresist that was used to make microfluidic channels out of polydimethylsiloxane and later using positive photoresist and etching to create a mold to make microfluidic channels out of polypropylene.

Summary of Research:

This research at the CNF has consisted of using microfabrication techniques to make a microfluidic device. Using the CAD software L-Edit, we make patterns to transfer to a mask using the Heidelberg mask writer. In the past year, we have made two types of masks: one for positive photoresist and the other for negative photoresist. The first set of microfluidic devices we made used the negative photoresist (SU-8) to make a mold.

The process of making a mold with photoresist (photolithography) consist of the steps; 1) Pour and spin photoresist onto a wafer (using CNF spinner), 2) Bake photoresist (using CNF hot plates), 3) Wait time, 4) Expose photoresist (using ABM contact aligner), 5) Second wait time, 6) Development photoresist. At the end of the process, we have a mold out of SU-8 on top of a wafer.

In the Kirby research group's lab, we made microfluidic devices by pouring PDMS on top of the mold, and then baking and attaching the molded PDMS to a glass slide through plasma cleaning. Unfortunately, for our application, we need the PDMS to be very hydrophobic and PDMS was not hydrophobic enough for these experiments. Therefore, we switched to making devices out of a polypropylene — a much more hydrophobic material.

To make the molded polypropylene pieces, we use hot embossing, which is done on the CNF hot press. Because of the large pressure applied during embossing, we needed a stronger mold than SU-8, so we switched to making molds out of silicon.

To make a mold out of silicon, a positive photoresist is spun instead of negative and after the photolithography process, the wafer is etched on the deep reactive ion etcher in the CNF. The mold is used in the CNF hot press to hot emboss the pattern onto polypropylene, which is then bonded using the hot press. We also used the CorSolutions microfluidic probe station for a time as a connection method for the tubes to the device. However, we determined that epoxy was a better method for the connecting tubes to the microfluidic device due to the pressure exerted by the CorSolution arm causing particles to clog.

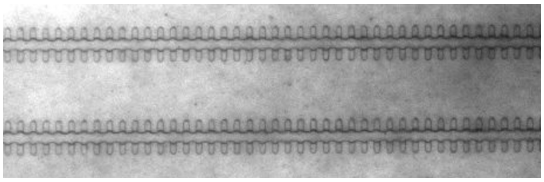

Figure 1: Developed positive resist pattern on wafer.

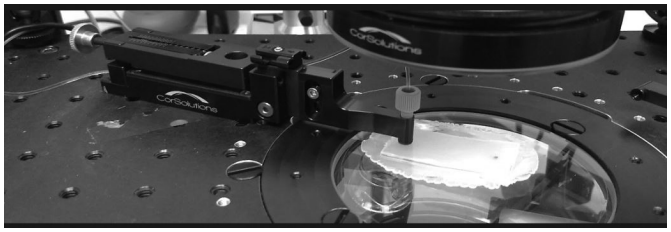

Figure 2: Embossed channels in polypropylene.

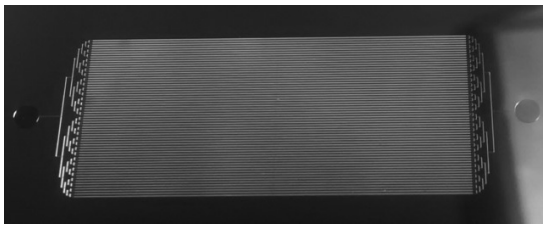

Figure 3: Device on CorSolutions microfluidic probe station.

Atomic-Scale Origami for the Fabrication of Micron Sized Machines

CNF Project Number: 2416-16

Principal Investigators: Itai Cohen, Paul L. McEuen

Users: Marc Z. Miskin, Baris Bircan, Edward P. Esposito, Tianyu Ma

Affiliations: Kavli Institute at Cornell for Nanoscale Science, School of Applied and Engineering Physics, Laboratory of Atomic and Solid-State Physics, Department of Physics; Cornell University

Primary Sources of Research Funding: National Science Foundation, Contract: DMR-1719875; Army Research Office, Contract: W911NF-18-1-0032

Contact: itai.cohen@cornell.edu, plm23@cornell.edu, mm2325@cornell.edu, bb625@cornell.edu, epe3@cornell.edu, tm478@cornell.edu

Primary CNF Tools Used: Oxford ALD FlexAL, Arradiance ALD Gemstar-6, Oxford 81 etcher, ABM contact aligner, SC 4500 odd-hour, Glen 1000 resist strip, Heidelberg DWL2000

Abstract:

Origami allows the creation of complicated three-dimensional structures from simple two-dimensional patterns. We are inspired to use origami for the fabrication of three-dimensional microscopic machines. The first step in such technology is the ability to fold thin sheets on-demand. Our work has demonstrated multiple mechanisms to actuate the folds in microscopic origami patterns, using standard processing techniques of the semiconductor industry.

Summary of Research:

Origami has emerged recently as a promising design strategy for creating arbitrarily complex three-dimensional structures from two-dimensionally patterned thin sheets [1,2]. As long as the two-dimensional pattern contains the proper array of mountain and valley folds, with a suitable actuation mechanism, we can create complicated three-dimensional origami structures that assemble themselves. Our work has demonstrated actuation mechanisms that works for nanometer-thin sheets, patterned using standard semiconductor processing technologies. This promises the smallest possible scale of origami devices.

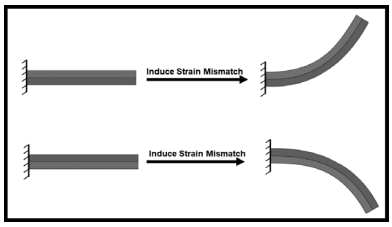

Figure 1: By introducing a strain mismatch between the bi-morph layers, we can cause a cantilever beam to bend.

Our devices rely on the bi-morph principle for actuation. One device, made from a stack with different materials in each of two layers, can be made to bend if the two layers strain by different amounts in response to an external stimulus, such as changing the temperature, or as in our previous work, the pH. Introducing a strain mismatch between the layers causes one layer to be in tension and the other to be in compression. By placing the bimorph stacks only in pre-specified regions, we can use the appropriate external stimulus to cause a thin sheet with an origami pattern to fold all at once.

Our prior work focused on bimorphs of silica (SiO_2) and graphene [3]. We first evaporate a sacrificial aluminum release layer onto a boro-silicate glass substrate, and then deposit a 2 nm layer of SiO_2 using the Oxford ALD FlexAL atomic layer deposition (ALD) tool. We then transfer graphene onto the SiO_2 layer, photolithographically pattern hinges and beams in any regions we would like to introduce a fold, and deposit pads of rigid SU-8 polymer over any regions we would like to remain flat. Finally, we remove the sacrificial aluminum layer with a wet etch to release our devices from the substrate into solution. Ion exchange causes the SiO_2 layer to swell.

Transferring graphene to the substrate is difficult and time-consuming as compared with deposition of an SiO_2 layer using the ALD tool, so it is beneficial to deposit both bimorph layers using ALD. We explored some of the materials available, and have settled on bimorph stacks of SiO_2 and silicon nitride (Si_3N_4), where each layer is 2 nm thick. The ion exchange mechanism is slightly different for the two layers, so lowering the pH still introduces a strain mismatch, causing cantilever beams to bend to roughly 10 μm radii of curvature, as in Figure

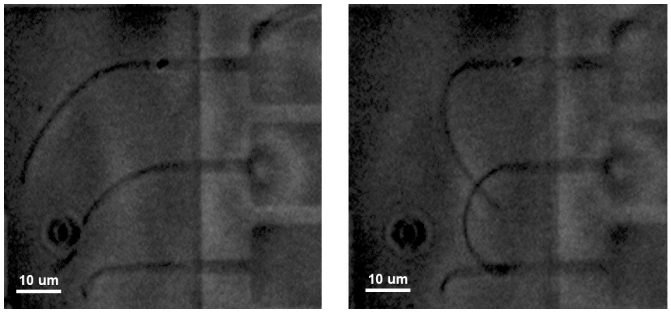

Figure 2: Bending of SiO_2 / Si_3N_4 bimorph cantilever beams by means of pH-induced ion exchange. Simply changing the solution from basic to acidic causes the beams to bend.

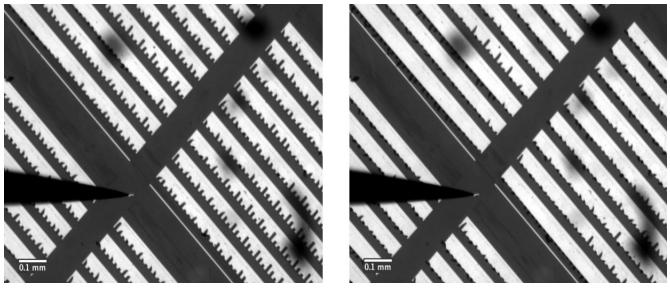

Figure 4: Applying a potential difference across an array of graphene / platinum bimorphs causes the entire array to fold at once.

2. Bimorphs with Si_3N_4 avoid some of the pre-stressing that occurs when using other materials.

Some work this year has focused on process development to allow us to use more sophisticated folding patterns. Devices fabricated with a single kind of bimorph stack are constrained to have all mountain or all valley folds, whereas most origami patterns require a single sheet to have both mountain and valley folds in different locations. We need devices capable of bi-directional folding. We have developed and refined a process that allows the fabrication of one bimorph stack together with the inverted bimorph stack as part of a single device, allowing beams with the two bi-morph stacks to fold into an S-shape, as in Figure 3. This has unlocked a whole realm of complex origami patterns. Professional origami artists have developed software that automatically generates design files we can include in mask designs.

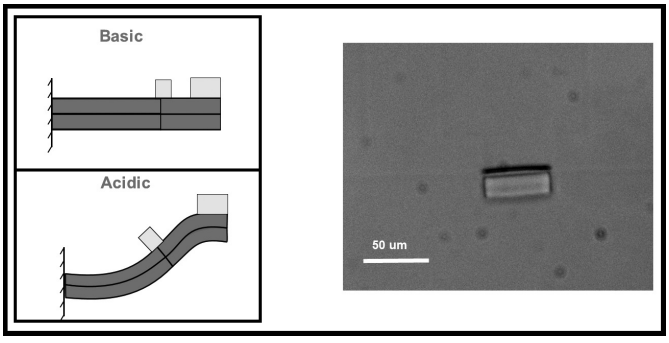

Figure 3: Schematic and experimental demonstration of bi-directional folding in SiO_2 / Si_3N_4 bimorph cantilever beams. The flat rectangle is a rigid SU-8 pad, parallel to the substrate, while the dark line above it is an SU-8 pad of the same size perpendicular to the substrate.

Our pH-based ion exchange mechanism allows us to change devices from the flat to the folded state at will, but it does not allow precise control over the radius of curvature in our devices when bent. As a promising new direction, part of our team has developed devices offering such precise control. Here, we use graphene with a 5 nm layer of platinum as our bimorphs. To actuate folds, we apply a voltage across our devices, and this potential difference allows ions from the solution to be absorbed into the platinum, swelling that layer as compared with the graphene, bending the device as before. By varying the applied potential difference, we can control the amount of bending, as shown in Figure 4. This technique allows an unprecedented control over the final three-dimensional configuration of our bending-actuated devices.

Our actuation mechanisms are well-suited for origami patterns in which all folds may be actuated at once. However, this is only a subset of all origami patterns. More complicated patterns require folds to be actuated in a specified sequence. Therefore, a major future direction of our work is to uncover techniques for actuating various folds sequentially.

References:

[1] Benbernou, N., Demaine, E. D., Demaine, M. L. and Ovadya, A. A universal crease pattern for folding orthogonal shapes. arXiv preprint arXiv:0909.5388 (2009).

[2] Felton, S., Tolley, M., Demaine, E., Rus, D. and Wood, R. A method for building self-folding machines. Science 345, 644-646 (2014).

[3] Miskin, M., Dorsey, K., Bircan, B., Han, Y., Muller, D., McEuen, P., and Cohen, I. Graphene-based bimorphs for micron-sized autonomous origami machines. Proceedings of the National Academy of Sciences, 115: 466-470 (2018).

A MEMS Repulsive Force Accelerometer

CNF Project Number: 2446-16

Principal Investigators: Shahrzad Towfighian, Ronald N. Miles

User: Mehmet Ozdogan

Affiliation: Mechanical Engineering Department, State University of New York at Binghamton

Primary Source of Research Funding: National Science Foundation Project ECCS grant # 1608692 titled "A New Approach to Capacitive Sensing: Repulsive Sensors"

Contact: stowfigh@binghamton.edu, rmiles@binghamton.edu, mozdoga1@binghamton.edu

Website: https://www.binghamton.edu/labs/mems/

Primary CNF Tools Used: Heidelberg mask writer - DWL2000, LPCVD N+/P+ polysilicon -wet oxide-CMOS nitride, MOS clean anneal, AS200 i-line stepper, Unaxis 770 deep Si etcher, Oxford 81-100 etchers, Logitech Orbis CMP, Zeiss Ultra SEM, SC4500 evaporator, RTA - AG610, DISCO dicing saw, Leica critical point dryer

Abstract:

This study reports fabrication and experimental characterization of a microelectromechanical systems (MEMS) capacitive accelerometer that utilizes repulsive force electrode configuration consisting of three fixed and one moving electrode. This configuration generates a net upward force on the moving electrode that is attached to a movable proof mass. The net force pushes the moving structure away from the substrate and produces an out-of-plane motion. Having this design comes with various benefits such as elimination of pull-in instability that severely limits functioning of electrostatic devices and causes permanent structural damages. This repulsive configuration concept has been investigated for actuator applications; however, it has not been employed for sensing purposes in the literature. Our goal is to create an accelerometer that works based on the repulsive sensing concept. The accelerometer is designed and fabricated with four-mask process. Following the fabrication, it is fixed on a shaker and tested under various DC bias and excitation levels to characterize its dynamic behavior. Laser Doppler Vibrometer (LDV) is used to measure its dynamic response under base excitation provided by the shaker. At 2.5 kHz excitation frequency, we measured the mechanical sensitivity of the sensor as 0.17, 0.13, and 0.09 μm/g at 40-50-60 V bias, respectively. Experimental results indicate that sensitivity of the accelerometer is the function of operating DC bias, excitation level and the excitation frequency. One can tune the sensitivity of the device by playing with these variables without experiencing pull-in instability, which is a great contribution.

Summary of Research:

The repulsive electrode configuration has been shown to be pull-in safe [1], which enables MEMS devices to have large travel ranges and proper functioning at high DC loads [2]. This method utilizes fringe electrostatic field to generate a net force that pushes away the proof mass from the substrate which eliminates the pull-in possibility. Main goal of this project is to exploit the benefits of utilizing repulsive electrode design in a capacitive sensor. The sensor design consists of fixed and moving electrodes which are attached to a rotating proof mass, see Figure 1. The design includes three sets of electrodes: grounded moving fingers, grounded aligned fixed fingers and voltage loaded unaligned fixed fingers. The moving and aligned fixed fingers are vertically separated with 2 μm initial gap.

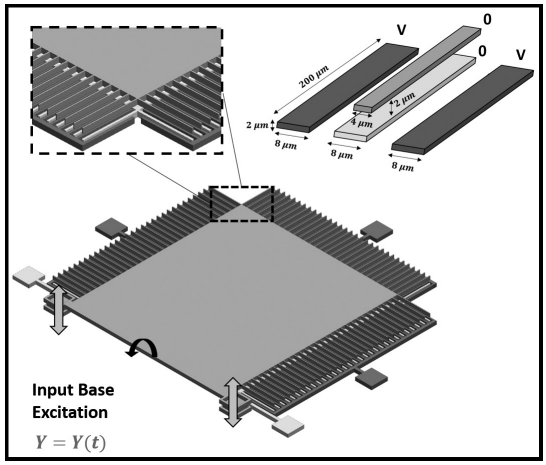

Figure 1: 3D model of the designed sensor showing the details of the proof mass and the electrodes.

The fabrication process flow of the accelerometer is shown in Figure 2. The process starts with a 100 mm silicon wafer. First, LPCVD silicon dioxide is grown as an insulation layer. Following this step,

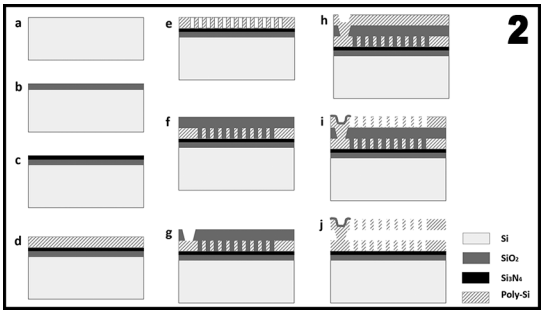

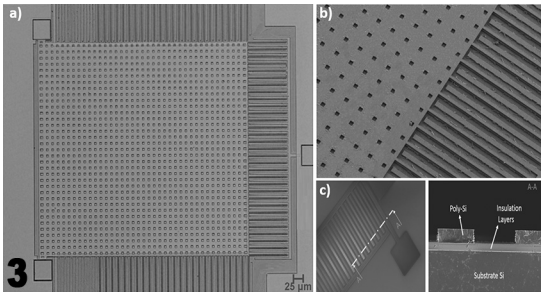

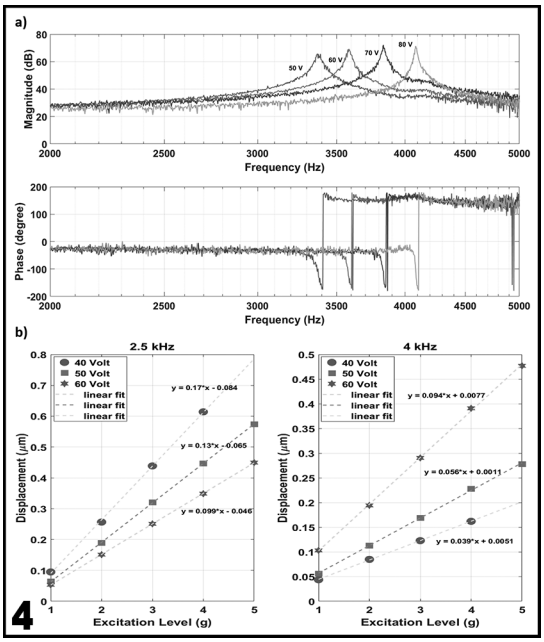

Figure 2, top: *Fabrication process flow of the sensor. (a) 4-inch, 525 μm thick silicon wafer. (b-c) Insulation layers growth and deposition, respectively. (d) First layer of 2 μm thick phosphorus doped polysilicon deposition. (e) RIE etch of polysilicon. (f) Sacrificial layer deposition and CMP processes. (g) Anchor etch on sacrificial layer. (h) Second 2 μm thick polysilicon deposition. (i) Polysilicon etch and gold deposition on the pads. (j) Proof mass release in HF:HCl mixture.* ***Figure 3, middle:*** *Images of the fabricated device. (a) Top view of the proof mass. (b) Moving and fixed fingers for the released device. (c) Fixed fingers and the cross-sectional view.* ***Figure 4, bottom:*** *Experimental results. (a) Shows the transfer function of the device which is performed to measure the resonance frequency of the sensor under various DC bias. (b) Shows the mechanical sensitivity (slope) of the sensor.*

LPCVD low stress silicon nitride is deposited on top of the oxide layer. After deposition of insulation layers first structural polysilicon layer is deposited using LPCVD furnace. Unaxis 770 plasma etcher is used to form fixed fingers out of this layer. On top of these fixed fingers, a sacrificial layer of LPCVD high-temperature-oxide (HTO) is deposited. Then, Logitech Orbis chemical mechanical polisher (CMP) is used to remove the step difference between fixed fingers and the proof mass. After the CMP process, vias are formed by etching the oxide layer using Oxford PlasmaLab 100 etcher. Later, second polysilicon layer is deposited and followed by annealing to reduce the residual film stresses. This layer is etched to form the proof mass attached with fingers and suspending torsional springs. Next, we deposit Cr and Au on the pads using evaporation tool SC4500 evaporator. After the evaporation process the wafers are diced and released in HF:HCl mixture. The fabricated device is presented in Figure 3.

The device is attached and wired to a PCB that is mounted on the head of a shaker. The device is excited in a vacuum environment. The side fingers are applied a DC bias while the shaker is vibrating with an AC harmonic signal which is the source of the base excitation. Laser Doppler vibrometer interfaced with data acquisition box is used to monitor the time-response of the device. The results are presented in Figure 4. Figure 4a shows the change of the resonance frequency of the device as the DC bias changes. Due to the fringe electrostatic forcing, as the DC load increases effective stiffness of the structure increases which results in shift of the resonance frequency. Figure 4b shows the relative motion of the proof mass when it is subjected to different excitation levels varying from 1g to 5g. Experimental results show that mechanical sensitivity (Figure 4b) of the device is the function of the applied DC bias and the frequency of the excitation. We are currently performing experiments to measure the response of the device to various shock impulses such as half-sine.

References:

[1] S. He and R. B. Mrad, "Design, Modeling, and Demonstration of a MEMS Repulsive-Force Out-of-Plane Electrostatic Micro Actuator", Journal of Microelectromechanical Systems, Vol. 17, no. 3, pp. 532-547, June 2008. doi: 10.1109/JMEMS.2008.921710.

[2] Towfighian S, He S, Ben Mrad R. "A Low Voltage Electrostatic Micro Actuator for Large Out-of-Plane Displacement.", ASME. IDETC/CIe, Vol. 4: doi:10.1115/DETC2014-34283.

Microfabrication of Micropillars inside a Microchannel

CNF Project Number: 2474-16

Principal Investigator: Dr. Yoav Peles

User: Faraz Khalil Arya

Affiliation: Mechanical and Aerospace Engineering, University of Central Florida

Primary Source of Research Funding: University of Central Florida Research Foundation Inc

Contact: yoav.peles@ucf.edu, arya@knights.ucf.edu

Primary CNF Tools Used: AutoCAD, AJA sputter deposition, photolithography processes, AJA ion mill

Abstract:

Boiling generates bubbles and predicting the movement of these bubble can be challenging. In this research, we fabricated micropillars and heaters in specific locations inside a microchannel and operate the heaters in calculated sequences. We moved the bubbles in the direction that we planned, and these movements pushed the liquid inside the channel toward the outlet.

Summary of Research:

The microfabrication process was conducted at the Cornell NanoScale Science and Technology Facility (CNF). Photolithography masks were designed and drew with AutoCAD and fabricated before they were taken to the CNF to be used during the fabrication process.

The fabrication was started on a Borofloat® wafer with the thickness of 500 μm and the diameter of 100 mm. Borofloat wafer was chosen because of the low heat conductivity (1.2 $W/(m \cdot K)^{-1}$), outstanding thermal resistance, very good temperature stability, excellent resistance to thermal shock, and a low coefficient of linear thermal expansion of around $3.25 \times 10^{-6}\ K^{-1}$.

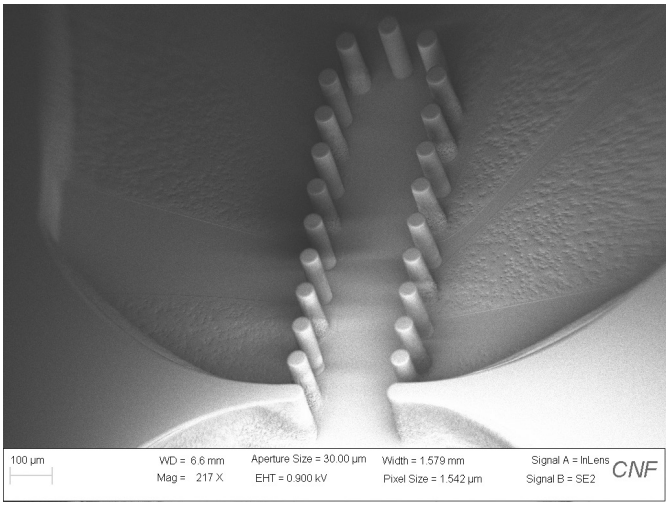

Figure 1: An image of the micropillar section of the microchannel that has been captured with a scanning electron microscope (SEM).

The Borofloat wafer was first cleaned with hot Piranha. After this step, the cleaned wafer was taken to the deposition tool so that 0.5 μm of Si_3N_4 was deposited on the substrate. This layer provides insulation between layers and acts as a mechanical isolation/buffer membrane. Depositing the vias and heaters was the next step.

The wafer was placed in the sputter deposition tool so that a 7 nm layer of titanium (Ti) could be deposited on it to enhance the deposition of a 30 nm layer of platinum (Pt). This layer of Pt is going to form the heaters of the device. Finally, a 1 μm layer of aluminum (Al) was deposited to provide the electrical connections. The first photolithography process was performed next and the excessive Al was removed by wet etching. After another photolithography process, the ion mill was used to etch the excess Pt and Ti. To insulate the heaters and vias layers from the flow inside the channel, a 1 μm layer of SiO_2 was deposited on the substrate. Contact pads should be the only parts of the wafer without the insulating layer of SiO_2, therefore, another process of photolithography was performed and the surplus SiO_2 layer was removed by dry etch.

To start the fabrication of the channel and the micropillars from SU-8, the wafer was first dehydrated in the oven. SU-8-100 was chosen as the appropriate SU-8 type and spun on the wafer in the spinning room. To conduct the soft bake step, the wafers were gradually heated up and kept at the temperature of 65°C for two hours and then baked at 95°C for a few more hours. The contact aligner was the selected tool to expose the SU-8 to the microchannel and micropillar designs that

were fabricated on the photolithography mask then a post exposure bake was carried out to prepare the SU-8 for development. The development phase included submerging the wafer upside down in SU-8 developer to remove the SU-8 from the unexposed part of the SU-8 layer. At the end of the SU-8 development process, the wafer was rinsed with isopropanol and SU-8 developer, and then blow dried with nitrogen.

To fabricate the top part of the device, double-coated film bonding tape was attached to a cleaned bare Borofloat wafer. A CO_2 laser machine drilled the holes into the top wafer by vaporizing the substrate. These holes were arranged in a way that after attaching to the bottom wafer, the contact pads would be accessible to operate the heaters. Next, the flow inlet and outlet on the bottom wafer were drilled. Top and bottom wafer was taken to the contact aligner once again to be attached to each other precisely. The final step in the fabrication process was cutting the wafer. A dicing saw was employed to cut the marked lines on the wafer to separate it into individual devices.

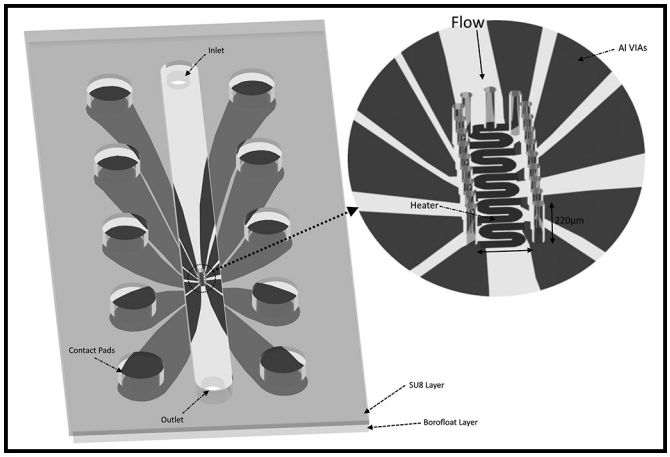

Figure 2: Schematic illustration of microchannel, which consists of arrays of micropillars within.